PERGAMON

International Journal of Solids and Structures 39 (2002) 5279–5293

INTERNATIONAL JOURNAL OF SOLIDS and STRUCTURES

www.elsevier.com/locate/ijsolstr

# Anisotropic damage model under continuum slip crystal plasticity theory for single crystals

Lu Feng *, Ke-shi Zhang, Guang Zhang, Hai-dong Yu

*Department of Applied Mechanics, Northwestern Polytechnical University, P.O. Box 169, Xi'an 710072, China*

Received 14 November 2001

**Abstract**

Modern concepts in the safe and economical design of components and structures need modern material models, which describe the material behavior more correctly. In high temperature design, the study of creep damage accumulation and its influence on the deformation behavior is very important. For ductile materials large deformation takes place at the level of damage appearance. Damage is anisotropic in nature. In this paper an anisotropic damage mechanics model based on a continuum damage mechanics (CDM) has been developed to model creep behavior of single crystal superalloys. Using the theory of CDM, the slip system model coupling with anisotropic damage model is developed. The model is formulated in the context of irreversible thermodynamics and the internal state variable theory. The distinguishing characteristic of the proposed constitutive model is that, by construction, the corresponding incremental stress–strain relations including damage evolution equation derive from a thermodynamical framework. The finite element program ABAQUS has been used and the slip system model is written using a user material subroutine. The numerical simulations show that the developed damage crystal model can reflect the microstructure such as the lattice orientation, self- and latent-hardening and rate sensitivity has great influence on the creep and damage development.



*Keywords:* Creep damage; Anisotropic damage; Crystal plasticity; Continuum damage mechanics

## 1. Introduction

Deterioration of an engineering component may occur in various ways depending on its operating environment and service loading conditions. It is a common phenomenon that at different service conditions, engineering components undergo creep deformation, which is accompanied by the nucleation, growth and coalescence of microcracks and microvoids, called creep damage. For inelastic analysis it is necessary consider material damage for designing components. As the creep damage has continuum property, continuum damage mechanics (CDM) recently find wide application to creep analysis for engineering

* Corresponding author. Tel.: +86-298-493-431x211.
*E-mail address:* lufengnwpu@yahoo.com (L. Feng).


PII: S0020-7683(02)00409-2

components and structures. During the past two decades much research has been concentrated modeling the progressive material degradation (material damage), which occurs prior to the initiation of a macroscopic crack.

In the classical continuum mechanics of solids, the elastic–plastic constitutive equations of a material satisfy the general thermodynamic principles under the assumption of a continuous material regardless of deformation amount. That is in the classical theory of plasticity, a material undergoes infinite plastic deformation without cracking since no criteria on the crack initiation and propagation are defined. Thus it cannot describe the global stiffness degradation due to microvoids and microcracks grown in the material during large deformation. In fracture mechanics, the energy dissipation during crack propagation and unstable sudden cracking can be estimated based on the assumption of prescribed initial cracks. As a consequence, the fracture mechanics approach focuses on the characteristic behaviors at the crack-tip zone for the given geometry of a crack. In circumstances where the defects are described in a statistically homogeneous manner, it is advantageous to model the mechanisms associated with material degradation within CDM, because both fracture and plasticity theories as well as other phenomenological material modeling approaches cannot treat material constitutive relations differently for virgin and damaged parts of a material at the same time.

CDM originated in the early works of Kachanov (1958) and Rabotnov (1968), who considered creep rupture of metals under uniaxial loading. Later, the concepts were extended to model fatigue (Chaboche and Lesne, 1988; Dufailly and Lemaitre, 1995), creep (Hayhurst, 1972; Cocks and Leckie, 1987) and ductile plastic damage (Lemaitre, 1985; Rousselier, 1987; Shin et al., 1997; Lämmer and Tsakmakis, 2000). Most of these concepts are embedded in the thermodynamics of irreversible processes and the internal state variable theory. To model isotropic damage processes, it suffices to define a scalar damage variable $D$, representing in some sense the progressive material degradation due to the loading process (Lemaitre and Chaboche, 1990). Ductile materials undergo large plastic deformation before fracture occurs. Damage due to initiation and growth of microvoids and microcracks is anisotropic in nature. Therefore the use of single parameter damage models, which assume isotropic damage, is strongly limited. Motivated by the results of microscopic investigations, a CDM-based anisotropic damage model has been developed. A second-order symmetric tensor is chosen in this model as the thermodynamic state variable describing the anisotropic damage. The damage evolution law is established under the thermodynamic restrictions. It is assumed that the tensile principal stresses are responsible for the damage growth, and the anisotrophy of the damage evolution depends on the principal directions of the stress and damage tensor. In this way, the damage-induced anisotrophy is also considered. For anisotropic damage, several models have been developed by Murakami and Ohno (1981), Chow et al. (1991) and Ju (1989).

Single crystal superalloys are of increasing importance, especially in the turbine industry. Viscoplastic damage approaches and life-time prediction under multi-dimensional loading conditions are of great interest. Mechanical properties of single crystal superalloys are strongly anisotropic and nonlinear. Recently much attention has paid on the development of constitutive models to describe deformation of superalloy single crystals. There have at least two ways on such aspect research. The first is the extension of phenomenological creep models to account for material anisotropy using orientation functions (Li and Smith, 1998; Qi and Bertram, 1998, 1999). Qi and Brocks (2000) developed a kind of anisotropic damage model which is coupled with the unified viscoplastic model to simulate the creep damage and deformation of single crystals at high temperatures. The second involves single crystal models considering slip on specific slip systems (Ghosh et al., 1990; Meric and Cailletaud, 1991; Jordan et al., 1993; Brehm and Glatzel, 1998; MacLachlan et al., 2001).

The work described here falls into the second way. An engineering component, which is operated at high temperatures for a long period of time, undergoes viscoplastic deformation and damage. The crystalline viscoplastic constitutive model, based on continuum slip theory find more and more application to the simulation of viscoplastic behavior of single crystals and polycrystals. However, it does not consider material damage. They are therefore not able to predict life time and to describe tertiary creep. According to the effective stress concept of CDM, an anisotropic damage model is coupled with the single crystal viscoplastic model by replacing the stress tensor in it by an adequate defined effective stress tensor. The model is formulated in the context of irreversible thermodynamics and the internal state variable theory. The distinguishing characteristic of the proposed constitutive model is that, by construction, the corresponding incremental stress–strain relations including damage evolution equation derive from a thermodynamical framework. Theoretical prediction of creep behavior and damage development for single crystal are presented and discussed.

A description of the notation used in the paper follows. Tensors and vectors will be denoted by bold-face letters (e.g. **F**, **T**). The following definitions for operation are used: $\mathbf{AB} = \mathbf{A}_{ik}\mathbf{B}_{kj}\mathbf{e}_i \otimes \mathbf{e}_j$, where $\otimes$ denotes the tensor product and $\mathbf{e}_i$ a Cartesian basis, $\mathbf{A} : \mathbf{B} = \mathbf{A}_{ij}\mathbf{B}_{ij}$. A superscript $-1$ indicates the inverse of a tensor, superscript T indicates its transpose and superscript $-$T indicates the transpose of its inverse.

## 2. Description of anisotropic damage

### 2.1. Isotropic damage in one-dimensional deformations

It is well-known that the creep process of metal is accompanied by the nucleation, growth and coalescence of microcracks. The simplest but widely accepted material damage is isotropic damage and fictitiously considered as the ratio of the reduced area to the cross-sectional area. Physically, isotropic damage consists of microcracks, microvoids and cavities with uniformly distributed orientation in all directions.

To model isotropic damage processes, scalar damage $D$ can be expressed as

$$D = \frac{A - A^*}{A} = 1 - \frac{A^*}{A} = 1 - \eta \tag{1}$$

where $A$ is the original, undamaged area and $A^*$ is the effective area after damage occurs. Then, the effective Cauchy stress ($\tilde{\sigma}$) which is the real stress acting on area $A^*$ can be written by

$$\tilde{\sigma} = \sigma/\eta = \sigma/(1 - D) \tag{2}$$

where $\sigma$ is the Cauchy stress. From a mathematical point of view, $D = 0$ characterizes the undamaged or virgin state, whereas $D = 1$ corresponds to the rupture of the element into two parts. Here for a one-dimensional state of stress, $\eta$ is a scalar quantity which cannot treat the dimensional characteristic of the internal damage. In the general case of three-dimensional deformations and damage, the nature and the definition of effective stress become more complex.

### 2.2. Anisotropic damage

A microcrack or microvoid has the directional characteristic in three-dimensional states of deformation. Thus, an isotropic damage model has limitations for multi-dimensional states of stress. It is widely recognized that the damage process in metals is generally anisotropic, even if the material is initially isotropic. For single crystals both the initial material anisotropy and the induced anisotropy due to damage must be taken into account. In the stress–strain relations of a material deteriorated by the evolution of damage, internal variables (damage variables) for the description of the material damage represents the stiffness variations. The predictive capabilities of a damage model depend strongly on its particular choice of damage variables. The geometrical properties of a given state of microcracks may be described, in a continuum sense, by a second-order symmetric tensor. This method has been widely used to represent anisotropic damage state in the anisotropic damage model proposed by Chow and Wang (1987a,b), which has been successfully employed to describe the creep and damage evolution of nickel-based superalloys in the high temperature regime by Qi and Bertram (1998, 1999).

The deformation behavior of material considering damage can be, according to the effective stress concept of CDM, described by any deformation constitutive equation when the stress tensor is replaced by an adequately defined effective stress tensor $\tilde{\boldsymbol{\sigma}}$. That means, the influence of both stress and damage state on the deformation behavior can be represented by a so-called effective stress. The effective stress in the present model is defined as:

$$\tilde{\boldsymbol{\sigma}} = (\mathbf{I} - \mathbf{D})^{-1/2} \cdot \boldsymbol{\sigma} \cdot (\mathbf{I} - \mathbf{D})^{-1/2} \tag{3}$$

where $\boldsymbol{\sigma}$ and $\mathbf{I}$ denote the stress tensor and the identity tensor of rank two, respectively.

### 2.3. Kinematics, strain and stress measure

Let $\mathbf{F}$ ($\det \mathbf{F} > 0$) be the deformation gradient tensor and

$$\mathbf{F} = \mathbf{F}^{\mathrm{e}} \cdot \mathbf{F}^{\mathrm{p}} \tag{4}$$

the multiplicative decomposition of $\mathbf{F}$ into elastic and plastic parts. $\mathbf{F}^{\mathrm{p}}$ is the plastic deformation gradient due to shearing along crystallographic slip planes, and $\mathbf{F}^{\mathrm{e}}$ is the elastic deformation gradient which includes any rigid rotation of the lattice. The transformation $\mathbf{F}^{\mathrm{p}}$ introduces a so-called plastic intermediate configuration denoted by $\widehat{R}_{\mathrm{t}}$. In the reference and current configuration the material body occupies the regions $R_{\mathrm{r}}$ and $R_{\mathrm{t}}$ in the three-dimensional Euclidean point space, respectively. For later reference, we introduce the relations

$$\mathbf{L}^{\mathrm{p}} = \dot{\mathbf{F}}^{\mathrm{p}}\mathbf{F}^{\mathrm{p}-1} \qquad \mathbf{D}^{\mathrm{p}} = \tfrac{1}{2}(\mathbf{L}^{\mathrm{p}} + \mathbf{L}^{\mathrm{pT}}) \tag{5}$$

Further, we denote by $\boldsymbol{\sigma}$ the Cauchy stress tensor, by $\boldsymbol{\tau}$ the weighted Cauchy stress tensor,

$$\boldsymbol{\tau} = (\det \mathbf{F})\boldsymbol{\sigma} \tag{6}$$

and by

$$\mathbf{T} = \mathbf{F}^{\mathrm{e}-1}\boldsymbol{\tau}\mathbf{F}^{\mathrm{e}-\mathrm{T}} \tag{7}$$

the second Piola–Kirchhoff stress tensor relative to $\widehat{R}_{\mathrm{t}}$.

The elastic behavior is modeled using a constitutive law written in the intermediate configuration,

$$\mathbf{T} = \boldsymbol{\xi} : \mathbf{E}^{\mathrm{e}} \tag{8}$$

where $\boldsymbol{\xi}$ is a fourth-order elasticity tensor. The elastic response was assumed to be isotropic, so that the elasticity tensor takes the form

$$\boldsymbol{\xi} = 2\mu\boldsymbol{\varpi} + \lambda(\mathbf{1} \otimes \mathbf{1})$$

where $\mu$ and $\lambda$ are Lamé's constants, and $\boldsymbol{\varpi}$ and $\mathbf{1}$ are the symmetric fourth-order and second-order identity tensors, respectively. The strain measure is given by the Green strain tensor $\mathbf{E}^{\mathrm{e}}$, defined as

$$\mathbf{E}^{\mathrm{e}} = \tfrac{1}{2}(\mathbf{C}^{\mathrm{e}} - \mathbf{I}) \qquad \mathbf{C}^{\mathrm{e}} = \mathbf{F}^{\mathrm{eT}}\mathbf{F}^{\mathrm{e}} \tag{9}$$

where $\mathbf{C}^{\mathrm{e}}$ is the elastic right Cauchy–Green tensor.

## 3. Thermodynamic framework of continuum damage mechanics

The characteristics of macroscopic behaviors of a material depend completely on the thermodynamics state of the material, which can be defined by a number of independent variables, i.e. state variables. The state variables are classified into two groups; one contains the observable variables that can be observed externally and the other contains the internal variables related to the deformation history and energy dissipation process, which cannot be measured by the current deformed state of deformation.

In the classical thermodynamics principles, the second law of thermodynamics provides the well-known Clausius–Duhem inequality in terms of state variables and the Helmholtz free energy density. However, in order to describe the mechanical energy dissipation process, especially for evolution equations of flux variables, a complementary formulation of Clausius–Duhem inequality could be applied. For this, the thermodynamic framework of the CDM approach proposed by Lemaitre and Chaboche (1990) is adopted in this study.

### *3.1. Effective elastic stiffness tensor*

For undamaged material, the elastic complementary energy is defined as

$$\mathbf{W}^{\mathrm{e}}(\boldsymbol{\sigma}) = \tfrac{1}{2}\boldsymbol{\sigma} : \boldsymbol{\xi}^{-1} : \boldsymbol{\sigma} \tag{10}$$

where $\boldsymbol{\xi}^{-1}$ is the inverse of elasticity tensor. According to the hypothesis of equivalence of elastic energy (Chow and Lu, 1989), the elastic energy of damaged material can be obtained as follows:

$$\mathbf{W}^{\mathrm{e}}(\boldsymbol{\sigma}, \mathbf{D}) = \tfrac{1}{2}\tilde{\boldsymbol{\sigma}} : \boldsymbol{\xi}^{-1} : \tilde{\boldsymbol{\sigma}} \tag{11}$$

### *3.2. Formulation of elastic–plastic damage constitutive equation*

In plastic damage problems, the hardening effect of a plastic deformation can be assumed to have no coupling effects with any other internal variables. Then the Helmholtz free energy $\boldsymbol{\psi}$ can be written in a decomposed form of elastic term $\boldsymbol{\psi}^{\mathrm{e}}$ and plastic term $\boldsymbol{\psi}^{\mathrm{p}}$ (Shin et al., 1997; Ortiz and Stainier, 1999)

$$\boldsymbol{\psi} = \boldsymbol{\psi}^{\mathrm{e}}(\mathbf{C}^{\mathrm{e}}, \mathbf{D}) + \boldsymbol{\psi}^{\mathrm{p}}(\boldsymbol{\gamma}^{\alpha}) \tag{12}$$

where

$$\boldsymbol{\psi}^{\mathrm{e}}(\mathbf{C}^{\mathrm{e}}, \mathbf{D}) = \tfrac{1}{2}\tilde{\boldsymbol{\sigma}} : \boldsymbol{\xi}^{-1} : \tilde{\boldsymbol{\sigma}} = \tfrac{1}{2}\mathbf{E}^{\mathrm{e}} : \boldsymbol{\xi} : \mathbf{E}^{\mathrm{e}} \tag{13}$$

Due to the restrictions of the principle of material frame indifference the elastic part of the Helmholtz free energy $\boldsymbol{\psi}^{\mathrm{e}}$ is formulated most generally in terms of the elastic right Cauchy–Green tensor $\mathbf{C}^{\mathrm{e}}$. For an account on this argument refer (e.g. Miehe and Stein, 1992). An additional scalar internal variable $\boldsymbol{\gamma}^{\alpha}$ is responsible for isotropic hardening and is the argument of the plastic part of the Helmholtz free energy $\boldsymbol{\psi}^{\mathrm{p}}$.

In view of isothermal deformation with uniform temperature distribution assumed in this paper, the Clausius–Duhem inequality is expressed in the effective second Piola–Kirchhoff stress tensor $\widetilde{\mathbf{T}}$ relative to $\widehat{R}_{\mathrm{t}}$ and plastic Lie derivative of the right Cauchy–Green tensor $\ell_{\mathbf{v}}^{\mathrm{p}}(\mathbf{C}^{\mathrm{e}})$ (Steinmann and Stein, 1996; Miehe et al., 1999)

$$\tfrac{1}{2}\widetilde{\mathbf{T}} : \ell_{\mathbf{v}}^{\mathrm{p}}(\mathbf{C}^{\mathrm{e}}) - \dot{\boldsymbol{\psi}} \geqslant 0 \tag{14}$$

Taking into account the definition of the plastic Lie derivative of the elastic right Cauchy–Green tensor (Steinmann and Stein, 1996; Miehe et al., 1999)

$$\ell_{\mathrm{v}}^{\mathrm{p}}(\mathbf{C}^{\mathrm{e}}) = \mathbf{F}^{\mathrm{p}-\mathrm{T}} \cdot \dot{\mathbf{C}} \cdot \mathbf{F}^{\mathrm{p}-1} = \dot{\mathbf{C}}^{\mathrm{e}} + 2[\mathbf{C}^{\mathrm{e}} \cdot \mathbf{L}^{\mathrm{p}}]^{\mathrm{sym}} \tag{15}$$

From Clausius–Duhem inequality (14) and using (12) and (13), we get

$$\frac{1}{2}\widetilde{\mathbf{T}} : \ell_{\mathrm{v}}^{\mathrm{p}}(\mathbf{C}^{\mathrm{e}}) - \dot{\boldsymbol{\psi}} = \frac{1}{2}\widetilde{\mathbf{T}} : \dot{\mathbf{C}}^{\mathrm{e}} + [\mathbf{C}^{\mathrm{e}} \cdot \widetilde{\mathbf{T}}] : \mathbf{L}^{\mathrm{p}} - \frac{\partial \boldsymbol{\psi}^{\mathrm{e}}}{\partial \mathbf{C}^{\mathrm{e}}} : \dot{\mathbf{C}}^{\mathrm{e}} - \sum_{\alpha} \frac{\partial \boldsymbol{\psi}^{\mathrm{p}}}{\partial \boldsymbol{\gamma}^{\alpha}} \dot{\boldsymbol{\gamma}}^{\alpha} - \frac{\partial \boldsymbol{\psi}^{\mathrm{e}}}{\partial \mathbf{D}} : \dot{\mathbf{D}} \geqslant 0 \tag{16}$$

In order to ensure that (16) is satisfied for every admissible process, we require

$$\widetilde{\mathbf{T}} = 2\frac{\partial \boldsymbol{\psi}^{\mathrm{e}}}{\partial \mathbf{C}^{\mathrm{e}}} = \boldsymbol{\xi} : \mathbf{E}^{\mathrm{e}} \tag{17}$$

and

$$[\mathbf{C}^{\mathrm{e}} \cdot \widetilde{\mathbf{T}}] : \mathbf{L}^{\mathrm{p}} - \sum_{\alpha} \frac{\partial \boldsymbol{\psi}^{\mathrm{p}}}{\partial \boldsymbol{\gamma}^{\alpha}} \dot{\boldsymbol{\gamma}}^{\alpha} - \frac{\partial \boldsymbol{\psi}^{\mathrm{e}}}{\partial \mathbf{D}} : \dot{\mathbf{D}} \geqslant 0 \tag{18}$$

We note that the elastic relationship (17) is similar to Eq. (8), while in (17) we have considered the damage that is different from Eq. (8). We define

$$\mathbf{g}^{\alpha} = \frac{\partial \boldsymbol{\psi}^{\mathrm{p}}}{\partial \boldsymbol{\gamma}^{\alpha}} \qquad \mathbf{Y}_{\mathrm{D}} = -\frac{\partial \boldsymbol{\psi}^{\mathrm{e}}}{\partial \mathbf{D}} \tag{19}$$

here $\mathbf{Y}_{\mathrm{D}}$ is the thermodynamic force associated with damage, called damage driving force. We have

$$\lfloor \mathbf{C}^{\mathrm{e}} \cdot \widetilde{\mathbf{T}} \rfloor : \mathbf{L}^{\mathrm{p}} - \sum_{\alpha} \mathbf{g}^{\alpha} \dot{\boldsymbol{\gamma}}^{\alpha} + \mathbf{Y}_{\mathrm{D}} : \dot{\mathbf{D}} \geqslant 0 \tag{20}$$

It can readily see that the inequalities

$$\mathbf{M} = \lfloor \mathbf{C}^{\mathrm{e}} \cdot \widetilde{\mathbf{T}} \rfloor : \mathbf{L}^{\mathrm{p}} - \sum_{\alpha} \mathbf{g}^{\alpha} \boldsymbol{\gamma}^{\alpha} \geqslant 0 \tag{21}$$

$$\mathbf{Y}_{\mathrm{D}} : \dot{\mathbf{D}} \geqslant 0 \tag{22}$$

are sufficient conditions for (20) to be satisfied.

To this end, the principle of maximum dissipation in its penalty formulation with $\dot{\gamma}_0$ a reference shear strain rate, i.e. the penalty parameter, and $\boldsymbol{\Phi}^{\alpha}(\ )$ monotonic increasing penalty functions is written as

$$-\mathbf{M}(\mathbf{C}^{\mathrm{e}} \cdot \widetilde{\mathbf{T}}, \mathbf{g}^{\alpha}) + \frac{1}{2}\sum_{\alpha} \dot{\gamma}_0 \boldsymbol{\Phi}^{\alpha}(\boldsymbol{\tau}^{\alpha}, \mathbf{g}^{\alpha}) \rightarrow \mathrm{sta} \tag{23}$$

with the Schmid resolved shear stress $\boldsymbol{\tau}^{\alpha}$ on slip system $\alpha$ which is characterized by the slip plane normal $\mathbf{N}^{\alpha}$ and slip direction $\mathbf{M}^{\alpha}$ in the plastic intermediate configuration, i.e.

$$\boldsymbol{\tau}^{\alpha} = [\mathbf{C}^{\mathrm{e}} \cdot \widetilde{\mathbf{T}}] : \mathbf{Z}^{\alpha} \quad \text{with} \quad \mathbf{Z}^{\alpha} = \mathbf{M}^{\alpha} \otimes \mathbf{N}^{\alpha} \tag{24}$$

$$\widetilde{\mathbf{T}} = \det(\mathbf{F}^{\mathrm{e}})\mathbf{F}^{\mathrm{e}-1}\widetilde{\boldsymbol{\sigma}}\mathbf{F}^{\mathrm{e}-\mathrm{T}} \tag{25}$$

Please note that plastic flow is assumed as plastic volume preserving since we have simple shear with $\mathbf{M}^{\alpha} \perp \mathbf{N}^{\alpha}$ for each crystallographic slip system $\alpha$. Typically, for FCC crystals we have $\alpha = 12$ octahedral slip systems all in the $\{1\,1\,1\}\langle 1\,0\,1\rangle$ slip family with $\mathbf{M}^\alpha$ parallel to $\langle 110\rangle$ and $\mathbf{N}^\alpha$ parallel to $\langle 1\,1\,1\rangle$ which may be activated in a three-dimensional deformation. Then the principle of maximum dissipation renders the associated flow rule for the plastic velocity gradient

$$\mathbf{L}^{\mathrm{p}} = \frac{1}{2}\sum_{\alpha}\dot{\gamma}_0 \partial_{\tau^\alpha}\mathbf{\Phi}^\alpha \mathbf{Z}^\alpha \underline{\underline{\mathrm{def}}} \sum_{\alpha}\dot{\gamma}^\alpha \mathbf{Z}^\alpha \tag{26}$$

Here,

$$\dot{\gamma}^\alpha = \tfrac{1}{2}\dot{\gamma}_0 \partial_{\tau^\alpha}\mathbf{\Phi}^\alpha \tag{27}$$

In the sequel the penalty function $\mathbf{\Phi}^\alpha$ are chosen in the sense of a Norton creep law as

$$\mathbf{\Phi}^\alpha = \frac{2\mathbf{g}^\alpha}{k+1}\left|\frac{\boldsymbol{\tau}^\alpha}{\mathbf{g}^\alpha}\right|^{(1/k)+1} \tag{28}$$

to render the evolution equations

$$\dot{\gamma}^\alpha = \dot{\gamma}_0\,\mathrm{sgn}(\boldsymbol{\tau}^\alpha)\left|\frac{\boldsymbol{\tau}^\alpha}{\mathbf{g}^\alpha}\right|^{1/k} \tag{29}$$

$$\boldsymbol{\tau}^\alpha = (\mathbf{C}^{\mathrm{e}} \cdot \widetilde{\mathbf{T}}) : \mathbf{Z}^\alpha \tag{30}$$

Often the hardening law is stated more generally in rate form for each slip system $\alpha$ (e.g. Asaro, 1979 or Hill, 1966 or Peirce et al., 1983), with $\mathbf{h}_{\alpha\beta}$ the hardening moduli as

$$\dot{\mathbf{g}}^\alpha(\gamma,\gamma^\beta) = \sum_{\beta}\mathbf{h}_{\alpha\beta}(\gamma)|\dot{\gamma}^\beta| \quad \text{with} \quad \dot{\gamma} = \sum_{\alpha}|\dot{\gamma}^\alpha| \tag{31}$$

and

$$\mathbf{h}_{\alpha\beta} = q\mathbf{h}(\gamma) + (1-q)\mathbf{h}(\gamma)\boldsymbol{\delta}_{\alpha\beta} \tag{32}$$

where

$$\mathbf{h}(\gamma) = h_0\,\mathrm{sech}^2\left(\frac{h_0\gamma}{\tau_{\mathrm{s}} - \tau_0}\right) \tag{33}$$

Now please note Eq. (22), in order to derive the constitutive equation without violating the second law of the thermodynamics, we introduce a simple expression of damage dissipation potential (Qi and Bertram, 1998, 1999)

$$\mathbf{\Phi}_{\mathrm{D}} = \tfrac{1}{2}\mathbf{Y}_{\mathrm{D}} : \overset{(4)}{\mathbf{S}} : \mathbf{Y}_{\mathrm{D}} \tag{34}$$

where $\overset{(4)}{\mathbf{S}}$ is a fourth-order tensor, called structure tensor. The damage evolution law is then given by

$$\dot{\mathbf{D}} = \frac{\partial \mathbf{\Phi}_{\mathrm{D}}}{\partial \mathbf{Y}_{\mathrm{D}}} = \overset{(4)}{\mathbf{S}} : \mathbf{Y}_{\mathrm{D}} \tag{35}$$

If the fourth-order tensor $\overset{(4)}{\mathbf{S}}$ is symmetric and positive-define, the thermodynamic restrictions will be automatically satisfied (Germain et al., 1983; Krajcinovic, 1983).

Note that the damage driving force is responsible for the evolution of damage. Damage development is affected by many factors. While current state of stress and damage mostly influence damage evolution. The influence of temperature is supposed to be represented by the temperature dependence of material parameters. The damage driving force for materials is postulated

$$\mathbf{Y}_{\mathrm{D}} = \langle \hat{\boldsymbol{\sigma}} \rangle^m = \sum_{i=1}^{3} \langle \hat{\boldsymbol{\sigma}}_i \rangle^m \hat{\mathbf{n}}_i^{\boldsymbol{\sigma}} \otimes \hat{\mathbf{n}}_i^{\boldsymbol{\sigma}} \tag{36}$$

where $m$ is a material parameter, $\hat{\boldsymbol{\sigma}}_i$ and $\hat{\mathbf{n}}_i^{\boldsymbol{\sigma}}$ are the $i$th eigenvector of the damage active stress $\hat{\boldsymbol{\sigma}}$ respectively, and $\langle \cdot \rangle$ are McCauley brackets.

Following the idea of effect stress, a so-called damage active stress tensor $\hat{\boldsymbol{\sigma}}$ is introduced to represent the effect of both stress and damage on the damage evolution. The damage active stress tensor is defined similarly to the effective stress tensor as:

$$\hat{\boldsymbol{\sigma}} = (\mathbf{I} - \mathbf{D})^{-n} \cdot \boldsymbol{\sigma} \cdot (\mathbf{I} - \mathbf{D})^{-n} = \sum_{i=1}^{3} \hat{\boldsymbol{\sigma}}_i \hat{\mathbf{n}}_i^{\boldsymbol{\sigma}} \otimes \hat{\mathbf{n}}_i^{\boldsymbol{\sigma}} \tag{37}$$

where $n$ is a material parameter, which is used to distinguish the effect of damage on the damage growth from the deformation rate.

Microscopic investigations show that the tensile principal stresses (not only the maximum principal stress) are responsible for the growth of microcracks and that the damage often develops perpendicularly to the principal directions of the stress tensor. It is therefore assumed that only the tensile damage active stresses are responsible for damage evolution, and the anisotropy of damage growth depends on the principal directions of the damage active stress tensor. The structure tensor in (35) is supposed to relate the material structure to damage. Consequently, the damage law (35) takes the following particular form:

$$\dot{\mathbf{D}} = \overset{(4)}{\mathbf{S}} : \mathbf{Y}_{\mathrm{D}} = A_0[\beta \mathbf{I} \otimes \mathbf{I} + (1 - \beta) \overset{(4)}{\mathbf{I}}] : \langle \hat{\boldsymbol{\sigma}} \rangle^m \tag{38}$$

where $A_0$, $\beta$ and $m$ are material parameters, and $\overset{(4)}{\mathbf{I}}$ denotes the fourth-order identity tensor. The structure tensor describes the isotropy–anisotropy behavior of damage evolution. It is easy to see that $\beta = 1$ corresponds to the totally isotropy damage evolution, and $\beta = 0$ totally anisotropic. (In this sense, the damage will develop perpendicularly to the principal damage active stresses and there is no isotropic part of damage.) Note that biaxial tests are needed for the determination of the anisotropy parameter $\beta$.

The damage law (38) can be rewritten as:

$$\dot{\mathbf{D}} = (\beta \mathbf{I} \otimes \mathbf{I} + (1 - \beta) \overset{(4)}{\mathbf{I}}) : \left\langle \frac{\hat{\boldsymbol{\sigma}}}{B_0} \right\rangle^m = (\beta \mathbf{I} \otimes \mathbf{I} + (1 - \beta) \overset{(4)}{\mathbf{I}}) : \sum_{i=1}^{3} \left\langle \frac{\hat{\boldsymbol{\sigma}}_i}{B_0} \right\rangle^m \hat{\mathbf{n}}_i^{\boldsymbol{\sigma}} \otimes \hat{\mathbf{n}}_i^{\boldsymbol{\sigma}} \tag{39}$$

This formulation is advisable for the identification of the material parameters. The new material parameter $B_0$ is used in (39) instead of $A_0$ in (38).

$$\dot{\mathbf{D}} = [\beta \mathbf{I} \otimes \mathbf{I} + (1 - \beta) \overset{(4)}{\mathbf{I}}] : \sum_{i=1}^{3} \left\langle \frac{\hat{\boldsymbol{\sigma}}_i}{B_0} \right\rangle^m \hat{\mathbf{n}}_i^{\boldsymbol{\sigma}} \otimes \hat{\mathbf{n}}_i^{\boldsymbol{\sigma}} \tag{40}$$

In summary, then, the crystal elastic–viscoplastic constitutive model coupling with anisotropic damage for large deformations can be written as:

- Crystal elastic–plastic constitutive model

$$\dot{\boldsymbol{\gamma}}^\alpha = \dot{\boldsymbol{\gamma}}_0 \operatorname{sgn}(\boldsymbol{\tau}^\alpha) \left| \frac{\boldsymbol{\tau}^\alpha}{\mathbf{g}^\alpha} \right|^{1/k}$$

- Hardening law

$$\dot{\mathbf{g}}^{\alpha}(\boldsymbol{\gamma}, \boldsymbol{\gamma}^{\beta}) = \sum_{\beta} \mathbf{h}_{\alpha\beta}(\boldsymbol{\gamma})|\dot{\boldsymbol{\gamma}}^{\beta}| \quad \text{with} \quad \dot{\boldsymbol{\gamma}} = \sum_{\alpha} |\dot{\boldsymbol{\gamma}}^{\alpha}|$$

$$\mathbf{h}_{\alpha\beta} = q\mathbf{h}(\boldsymbol{\gamma}) + (1-q)\mathbf{h}(\boldsymbol{\gamma})\boldsymbol{\delta}_{\alpha\beta}$$

$$\mathbf{h}(\boldsymbol{\gamma}) = h_0 \operatorname{sech}^2\left(\frac{h_0\boldsymbol{\gamma}}{\tau_s - \tau_0}\right)$$

- Effective stress

$$\hat{\boldsymbol{\sigma}} = (\mathbf{I} - \mathbf{D})^{-n} \cdot \boldsymbol{\sigma} \cdot (\mathbf{I} - \mathbf{D})^{-n} = \sum_{i=1}^{3} \hat{\boldsymbol{\sigma}}_i \hat{\mathbf{n}}_i^{\boldsymbol{\sigma}} \otimes \hat{\mathbf{n}}_i^{\boldsymbol{\sigma}}$$

$$\tilde{\boldsymbol{\sigma}} = (\mathbf{I} - \mathbf{D})^{-1/2} \cdot \boldsymbol{\sigma} \cdot (\mathbf{I} - \mathbf{D})^{-1/2}$$

- Damage evolution law

$$\dot{\mathbf{D}} = [\beta\mathbf{I} \otimes \mathbf{I} + (1-\beta)\overset{(4)}{\mathbf{I}}] : \sum_{i=1}^{3} \left\langle \frac{\widehat{\boldsymbol{\sigma}}_i}{B_0} \right\rangle^m \hat{\mathbf{n}}_i^{\boldsymbol{\sigma}} \otimes \hat{\mathbf{n}}_i^{\boldsymbol{\sigma}}$$

- Elastic constitutive law

$$\widetilde{\mathbf{T}} = \boldsymbol{\xi} : \mathbf{E}^{\mathrm{e}}$$

$$\widetilde{\mathbf{T}} = \det(\mathbf{F}^{\mathrm{e}})\mathbf{F}^{\mathrm{e}-1}\tilde{\boldsymbol{\sigma}}\mathbf{F}^{\mathrm{e}-\mathrm{T}}$$

## 4. Numerical calculations and discussions

In order to verify the validity of the proposed constitutive model, a non-linear large strain problem is considered. The proposed single crystal elasto-viscoplastic damage evolution equations are incorporated into the ABAQUS finite element software.

In the work by Qi and Brocks (2000), the material parameters of Chaboche model for IN 738LC at 850 °C determined by Olscheqski et al. are given and three creep test curves are presented. Elastic moduli $E = 149.65$ GPa, Poisson's ratio $\gamma = 0.33$. The material parameters of crystal plasticity for IN 738LC at 850 °C are estimated by trial calculation and they are: $k = 0.05$, $\tau_0 = 230$ MPa, $\tau_s = 265$ MPa, $h_0 = 2200$ MPa, $q = 1.0$. The corresponding material parameters of the damage model are adopted from the work of Qi and Brocks (2000) ($\beta = 0.5$, $n = 0.4$, $B_0 = 1280$ MPa, $m = 12$). The test curves and simulation curves using the proposed model are showed in Fig. 1.

Next we simulate the creep strains with and without damage under various constant loads for the three extreme orientations. The influence of the crystal orientation on the mechanical behavior was the most striking characteristic of single crystals. Figs. 2–4 show the simulated strains of the creep and damage development by using the single crystal model with damage under various constant loads for [0 0 1], [0 1 1] and [1 1 1] orientations, respectively. Note that the time scale of the figures for different orientations differs widely. These figures show that the used damaged model can reflect the anisotropic damage development and its influence on the anisotropic creep behavior.

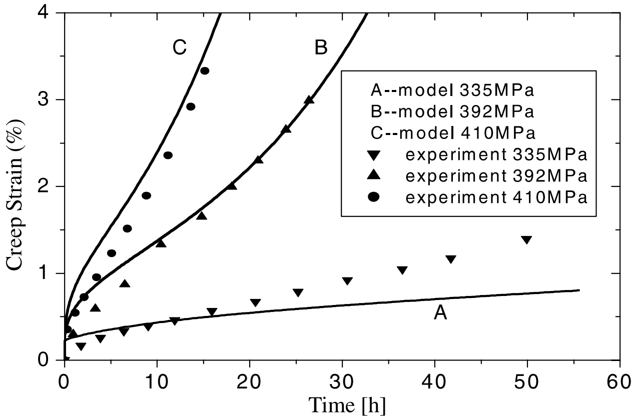


Fig. 1. Experiments and model predictions.

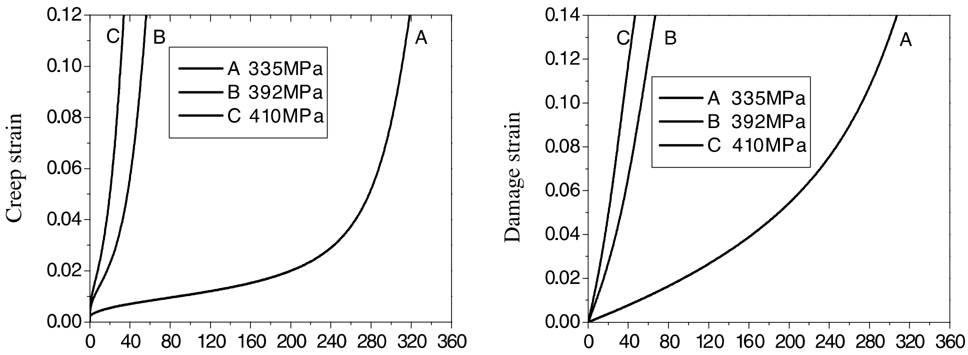


(a) Time [h] (b) Time [h]

Fig. 2. Creep modeling coupling with damage for [0 0 1] orientation.

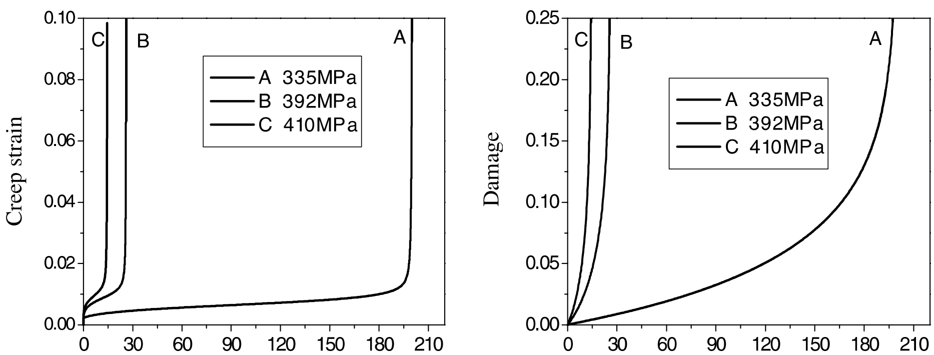


(a) Time [h] (b) Time [h]

Fig. 3. Creep modeling coupling with damage for [0 1 1] orientation.

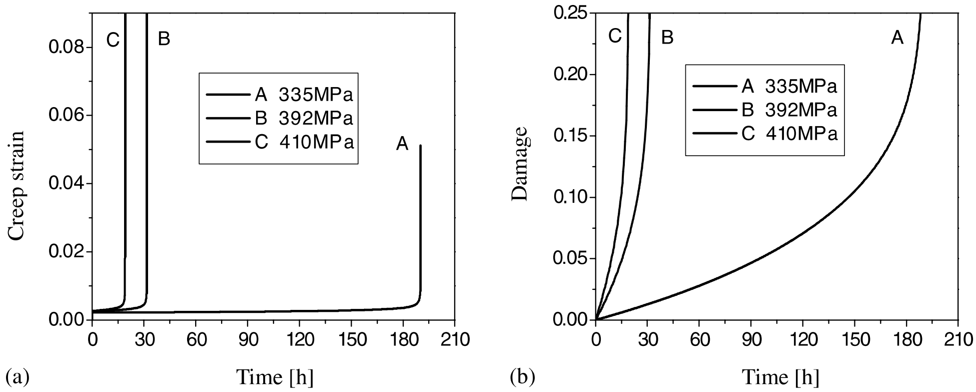


Fig. 4. Creep modeling coupling with damage for [1 1 1] orientation.

Comparison the results of the calculations by the model with and without damage are shown in Figs. 5–7 for three orientations. It can be seen from these curves that the creep rate calculated by the present model is always larger than the one calculated by the model without respect to material damage. The effective stress increases during the loading process and thus causes the material damage development. The coupled model with damage simulates the complete creep behavior till rupture, and can be used for the prediction of life time.

There is strong microstucture evidence that the significant components of the hardening matrix should be those causing self- and latent-hardening of the slip systems (MacLachlan et al., 2001). Our numerical simulation draw the same conclusion. Figs. 8 and 9 show the creep strains and damage development for three values of the latent hardening ratio $q$ for [0 0 1] orientation and [0 1 1] orientation respectively. The large value of $q$ means the strong influence of latent hardening. We can see from these curves that the values of $q$ have great influence on the creep properties of single crystals. When loading along different orientation the influence of latent hardening on the development of creep and damage is different.

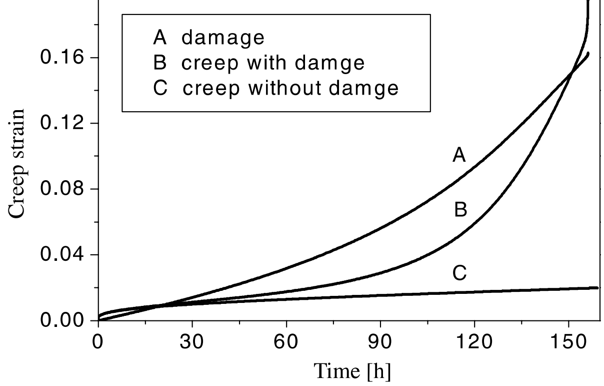


Fig. 5. Comparison between creep model and creep model coupling with damage for [0 0 1] orientation ($\sigma = 360$ MPa).

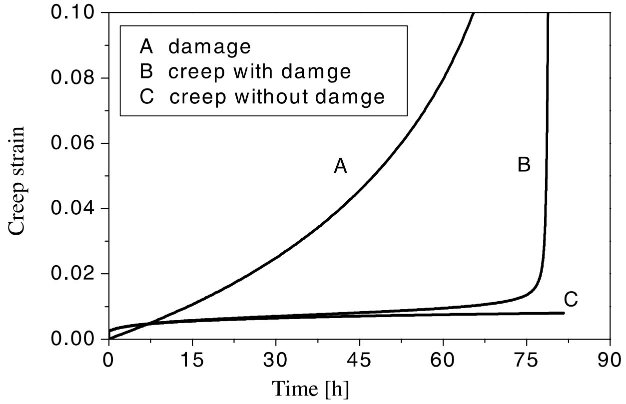


Fig. 6. Comparison between creep model and creep model coupling with damage for [0 1 1] orientation ($\sigma = 360$ MPa).

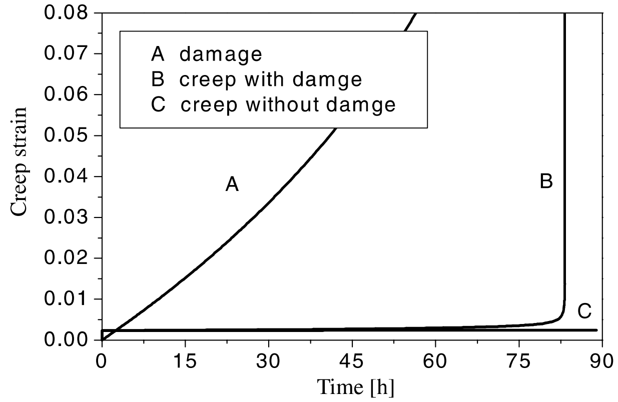


Fig. 7. Comparison between creep model and creep model coupling with damage for [1 1 1] orientation ($\sigma = 360$ MPa).

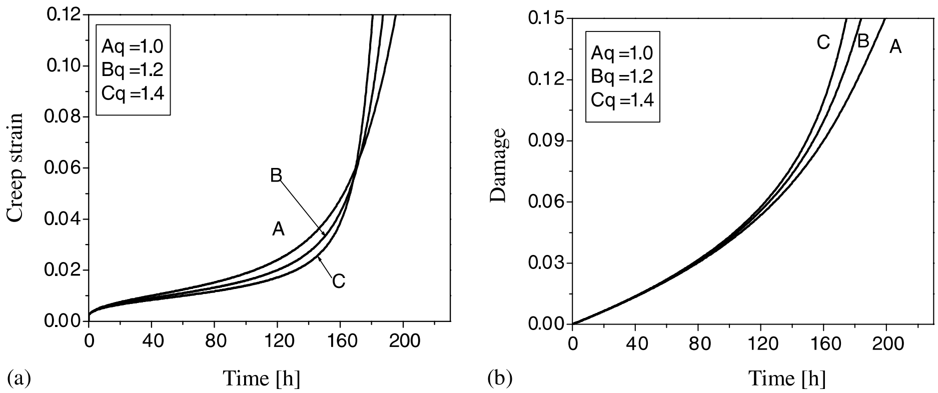


Fig. 8. Creep strains and damage development for three values of the latent hardening ratio $q$ for [0 0 1] orientation ($\sigma = 350$ MPa).

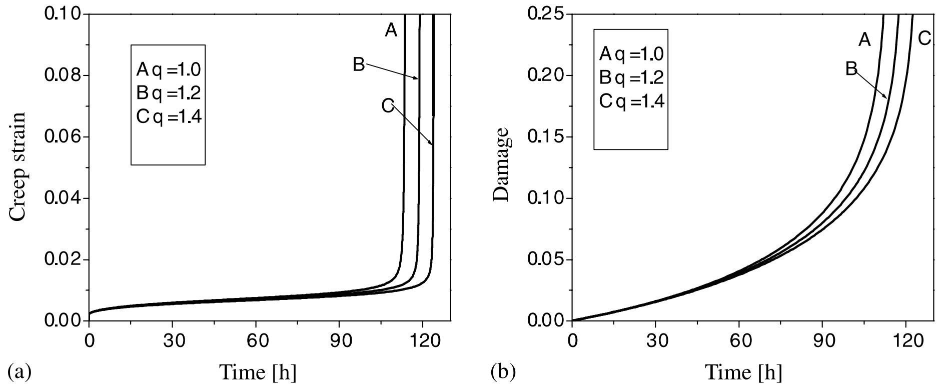


Fig. 9. Creep strains and damage development for three values of the latent hardening ratio $q$ for [0 1 1] orientation ($\sigma = 350$ MPa).

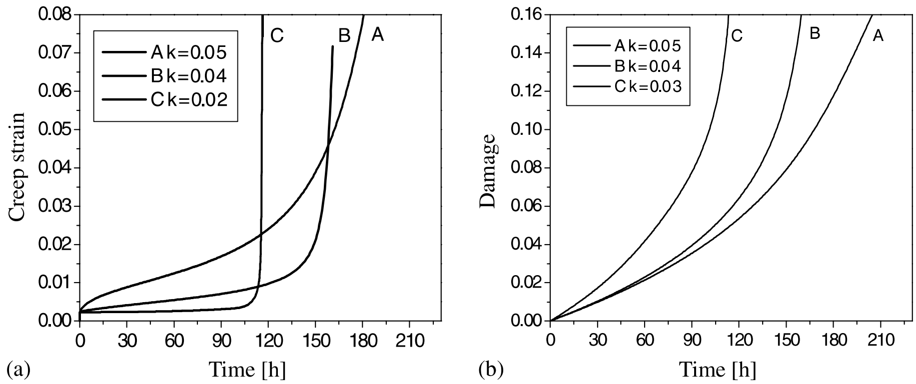


Fig. 10. Creep strains and damage development for three values of the latent hardening ratio $m$ for [0 0 1] orientation ($\sigma = 350$ MPa).

The effects of rate sensitivity are also explored in calculations. For the crystal model described above it is found that the strain rate sensitivities of single crystals have very significant effects on the development of creep. Fig. 10 shows the creep strain curves for three different values of $k$. It is found that increasing $k$ causes a significant increase in the creep strain and damage development. This demonstrates that rate sensitivities which might easily be ignored in the analysis have noticeable influence on the creep and damage development.

Recent measurements of lattice rotations occurring during single crystal creep at different orientations using electron back scattered diffraction technique have indicated that the activate slip systems at different temperature are different (Kakehi, 2000; MacLachlan et al., 2001). In present research we only consider $\{1\,1\,1\}\langle 1\,0\,1\rangle$ family of slip system. But the model can easily be extended to more family of slip system such as $\{1\,1\,1\}\langle 1\,1\,2\rangle$ systems.

While no attempt has been made here to quantitatively match the results of the simulation with experimental result, it has been shown that the material model proposed here can capable of qualitatively predicting the microstructure of single crystals such as the lattice orientation, self- and rate-sensitivity has great influence on the creep and damage development.

## Acknowledgements

This research was initiated with the support from National Natural Science Foundation of China and the Doctorated Foundation of Northwestern Polytechnical University.


## References


Asaro, R.J., 1979. Geometrical effects in the inhomogeneous deformation of ductile single crystals. Acta Metall. 27, 445–453.

Brehm, H., Glatzel, U., 1998. Material model describing the orientation dependent creep behavior of single crystals based on dislocation densities of slip systems. Int. J. Plast. 15, 285–298.

Chaboche, J., Lesne, P., 1988. A non-linear continuous fatigue damage model. Fatigue Fract. Engng. Mater. Struct. 11, 1–17.

Chow, C.L., Lu, T.J., 1989. On evolution laws of anisotropic damage. Engng. Fract. Mech. 3 (3), 679–701.

Chow, C.L., Wang, J., 1987a. An anisotropic theory of continuum damage mechanics for ductile fracture. Engng. Fract. Mech. 27 (5), 547–558.

Chow, C.L., Wang, J., 1987b. An anisotropic theory of elasticity for continuum damage mechanics. Int. J. Fract. 33, 3–16.

Chow, C.L., Liu, Y.J., Asundi, A., 1991. An incremental stress-based constitutive modeling on anisotropic damaged materials. Int. J. Fract. 47, 145–160.

Cocks, A., Leckie, F., 1987. Creep constitutive equations for damaged materials. Adv. Appl. Mech. 25, 239–294.

Dufailly, J., Lemaitre, J., 1995. Modeling very low cycle fatigue. Int. J. Damage Mech. 4, 153–170.

Germain, P., Nguyen, Q.S., Suquet, P., 1983. Continuum thermodynamics. J. Appl. Mech. 50, 1010–1020.

Ghosh, R.N., Curtis, R.V., Mclean, M., 1990. Creep deformation of single crystal superalloys-modeling the crystallographic anisotropy. Acta Metall. Mater. 38 (10), 1977–1992.

Hayhurst, D., 1972. Creep rupture under multiaxial states of stress. J. Mech. Phys. Solids 20, 381–390.

Hill, R., 1966. Generalized constitutive relations for incremental deformation of metal crystal by multislip. J. Mech. Phys. Solids 14, 95–102.

Jordan, E.H., Shixiang, S., Walker, K.P., 1993. The viscoplastic behaviour of HASTELLOY-X single crystal. Int. J. Plast. 9, 119–139.

Ju, J.W., 1989. On energy-based coupled elastoplastic damage theories: constitutive modeling and computational aspects. Int. J. Solid Struct. 25 (7), 803–833.

Kachanov, L., 1958. Time of the rupture process under creep conditions. Izv. Akad. Nauk. SSR 8, 26–31.

Kakehi, K., 2000. Effect of plastic anisotropy on the creep strength of single crystals of a nickel-based superalloy. Metall. Mater. Trans. A 31A, 421–430.

Krajcinovic, D., 1983. Constitutive equations for damaging materials. J. Appl. Mech. 50 (6), 355–360.

Lämmer, H., Tsakmakis, Ch., 2000. Discussion of coupled elastoplasticity and damage constitutive equations for small and finite deformations. Int. J. Plast. 16, 495–523.

Lemaitre, J., 1985. A continuous damage mechanics model for ductile fracture. J. Engng. Mater. Technol. 107, 83–89.

Lemaitre, J., Chaboche, J.L., 1990. Mechanics of Solid Materials. Cambridge University Press, Cambridge.

Li, S.X., Smith, D.J., 1998. Development of an anisotropic constitutive model for single crystal superalloy for combined fatigue and creep loading. Int. J. Mech. Sci. 40 (10), 937–938.

MacLachlan, D.W., Wright, L.W., Gunturi, S., Knowles, D.M., 2001. Constitutive modeling of anisotropic creep deformation in single crystal blade alloys SRR99 and CMSX-4. Int. J. Plast. 17, 441–467.

Meric, L., Cailletaud, G., 1991. Single crystal modeling for structural calculations: part 1—model presentation. J. Engng. Mater. Technol. 113, 171–182.

Miehe, C., Stein, E., 1992. A canonical model of multiplicative elasto-plasticity: Formulation and aspects of the numerical implementation. Eur. J. Mech. A/Solids 11, 25–43.

Miehe, C., Schröder, J., Schotte, J., 1999. Computational homogenization analysis in analysis in finite plasticity simulation of texture development in polycrystalline materials. Comput. Meth. Appl. Mech. Engng. 171, 387–418.

Murakami, S., Ohno, N., 1981. A continuum theory of creep and creep damage. In: Ponter, A.R.S., Hayhurst, D.R. (Eds.), 3rd IUTAM Symposium on Creep in Structures. Springer-Verlag, Berlin, pp. 422–444.

Peirce, D., Asaro, R.J., Needleman, A., 1983. Material rate dependence and localized deformation in crystalline solids. Acta Metall. 31 (12), 1951–1976.

Steinmann, P., Stein, E., 1996. On the numerical treatment and analysis of finite deformation ductile single crystal plasticity. Comput. Mech. Engng. 129, 235–254.

Rabotnov, Y., 1968. Creep rupture. In: Hetenyi, M., Vincenti, W. (Eds.), Applied Mechanics. Proceedings of the 12th International Congress of Applied Mechanics, 26–31 August 1968, Stanford. Springer-Verlag, Berlin, pp. 342–349.

Rousselier, G., 1987. Ductile fracture models and their potential in local approach of fracture. Nucl. Engng. Des. 105, 97–111.
Shin, I.G., Nho, I.S., Yim, S.J., 1997. A finite element approach to anisotropic damage of ductile materials in large deformations. Int. J. Fract. 84, 261–277.
Qi, W., Bertram, A., 1998. Damage modeling of the single crystal superalloy SRR99 under monotonous creep. Comput. Mater. Sci. 13, 132–141.
Qi, W., Bertram, A., 1999. Anisotropic continuum damage modeling for single crystals at high temperatures. Int. J. Plast. 15, 1197–1215.
Qi, W., Brocks, W., 2000. Simulation of anisotropic creep damage in engineering components. ECCOMAS 2000, 1–14.